

## Supporting Information

### **Defect engineering synthesis of oxygen doped carbon nitride microtubules for enhanced visible-light-driven photocatalysis**

Li Zhou,<sup>a</sup> Menghan Xu,<sup>a</sup> Wenjie Zhang,<sup>a</sup> and Xiaoquan Yao,<sup>\*a</sup>

---

Department of Applied Chemistry, School of Material Science and Technology, Nanjing University of Aeronautics and Astronautics, Nanjing 210016, P. R. China.

---

\*Corresponding author:

E-mail addresses: yaoxq@nuaa.edu.cn (X. Yao)

---

## Table of Contents

<b>Experimental section</b>	Chemicals and materials	S3
<b>Experimental section</b>	Measurement and Characterization	S3
<b>Figure S1.</b>	The EDX element distribution mapping of C、N and O in OCN	S5
<b>Table S1.</b>	Element content table of OCN	S6
<b>Figure S2.</b>	Photocatalytic degradation of TC by OCN synthesized with different amounts of hydrogen peroxide	S7
<b>Figure S3.</b>	Photocatalytic degradation of tetracycline by pH of different solutions	S8
<b>Figure S4.</b>	Photocatalytic degradation of tetracycline by catalysts of different quality	S9
<b>Figure S5.</b>	Photocatalytic degradation of tetracycline at different mass concentrations	S10
<b>Figure S6.</b>	Stability experiments of photocatalytic degradation of tetracycline of OCN	S11
<b>Figure S7.</b>	XRD patterns after cycles of OCN	S12
<b>Figure S8.</b>	SEM images of OCN after cycles	S13
<b>Figure S9.</b>	The rate of hydrogen production from photocatalytic water.	S14

---

## **Experimental section:**

### **2.1. Chemicals and materials**

In this research, Melamine (MA,  $C_3H_6N_6$ , 99%), Hydrogen peroxide ( $H_2O_2$ , 30%) and Acetonitrile ( $C_2H_3N$ , 99%) were provided by Beijing Inno Chem Science & Technology Co., Ltd. Tetracycline ( $C_{22}H_{24}N_2O_8$ , abbreviated as TC, 98%) and chloroplatinic acid hydrate ( $H_2PtCl_6 \cdot 6H_2O$ , 99.9%) were purchased from Aladdin. Triethanolamine ( $C_6H_{15}NO_3$ , 99%), L-Ascorbic acid ( $C_6H_8O_6$ , 99%), and isopropanol ( $C_3H_8O$ , 99%) were purchased from Macklin Co., Ltd. All other chemical reagents involved were of analytical grade and employed without further purification. Meanwhile, deionized water ( $>18.2 \text{ M}\Omega \cdot \text{cm}$ ) was obtained from a Milli-pore Milli-Q system (High-tech, Shanghai) and used throughout the experiments.

All instruments and characterisations adopted in this experiment are detailed in the “Supporting Information” section.

### **2.2 Measurement and Characterization**

The crystal phase, photoelectric properties, elemental compositions, and morphologies were performed using an X-ray diffraction (XRD) spectroscope (Bruker D8 ADVANCE), UV–vis spectroscopy (JP Shimadzu Co., Ltd), scanning electron microscope (SEM) (Mira 4, Tescan) with energy-dispersed spectroscopy (EDS, Oxford Ultim Max65), and X-ray photoelectron spectroscopy (XPS) (250Xi, Thermo Fisher). Fourier transform infrared spectra (FT-IR) were analyzed by Thermo Scientific Nicolet iS20. The specific surface areas were determined with a surface area analyzer (ASAP 2020 Micropore System, Micromeritics Instrument Corporation, USA) by the Brunauer-Emmett-Teller (BET) method. Steady-state photoluminescence (PL) and time-resolved photoluminescence (TRPL) spectra were recorded using a spectroscopic instrument (FLS1000, Edinburgh Instruments Ltd., UK) with an excitation wavelength of 375 nm at room temperature. A 375 nm laser in timecorrelated single-photon counting (TCSPC) mode was used to measure the decay lifetime of the PL spectra. The generation of superoxide radicals ( $\bullet O_2^-$ ) was verified by electron paramagnetic resonance EPR (Bruker E500, Bruker BioSpin GmbH)

---

measurements using 5,5-dimethyl-1-pyrroline N-oxide (DMPO) as the spin-trapping agent.

**Photoelectrochemical Measurement:** Photoelectrochemical tests were conducted in a conventional three-electrode cell at room temperature and pressure using an electrochemical workstation (CHI660D, Shanghai, China). The electrolyte used was 0.5 M Na<sub>2</sub>SO<sub>4</sub>, with the Ag/AgCl reference electrode, the Pt counter electrode, and the working electrode of the samples under investigation. 2 mg of the sample was added to 180 μL of ethanol and 20 μL of Nafion and mix with ultrasound. The solution was mixed and drop-cast onto FTO glass with a fixed area (1 cm<sup>2</sup>). The electrode was dried to obtain the working electrode for subsequent testing. Transient photocurrent measurements were recorded at a potential of 0.4 V (versus Ag/AgCl) under irradiation from a 300 W xenon lamp equipped with a simulated solar filter.

**Photocatalytic hydrogen evolution from water splitting:** In the photodeposition process of Pt (0.5 wt %) on the sample, 40 mg of the sample was dispersed through ultrasonication in a methyl alcohol aqueous solution (V<sub>water</sub>:V<sub>methanol</sub>=55 mL : 15 mL) within a reaction cell. Subsequently, a solution of H<sub>2</sub>PtCl<sub>6</sub>·6H<sub>2</sub>O at a concentration of 0.5 M was added to the reaction cell. The system was then connected to the evaluation system. The evaluation of photocatalytic overall water splitting performance, was conducted in a closed gas circulation system equipped with an overhead-irradiation-type glass vessel. Prior to each test, all the air should be removed and 1 kPa Ar was injected for facilitating the detection of little generated gases. A 300 W Xe lamp was adopted as the irradiation source (equipped with a 420 nm cut-off filter). During each reaction, the suspension was kept at 25 °C, and the evolved gases were analyzed by gas chromatography (GC-2014c).

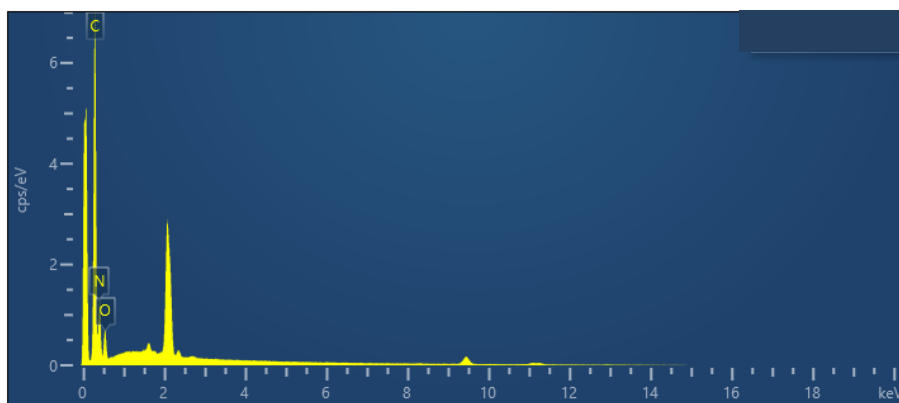


**Fig S1.** The EDX element distribution mapping of C、 N and O in OCN

---

**Table S1.** Element content table of OCN

<b>Element</b>	<b>Wt%</b>	<b>Wt% Sigma</b>	<b>At%</b>
C	51.09	0.36	55.6
N	38.32	0.40	35.76
O	10.59	0.20	8.65
total	100.00		100.00

---

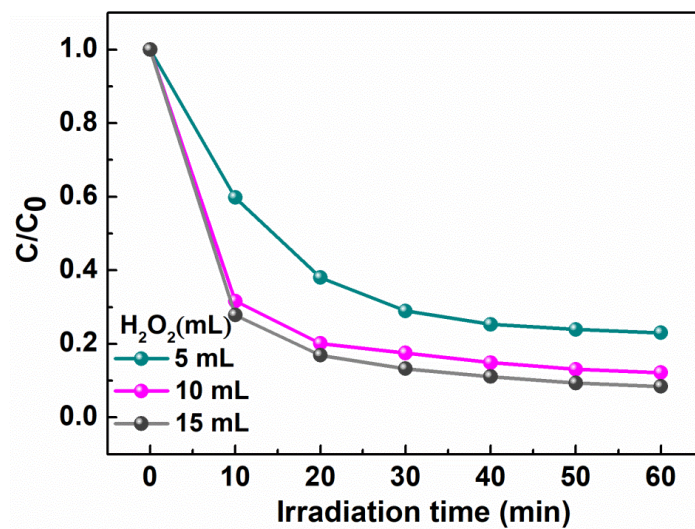


**Fig S2.** Photocatalytic degradation of TC by OCN synthesized with different amounts of hydrogen peroxide

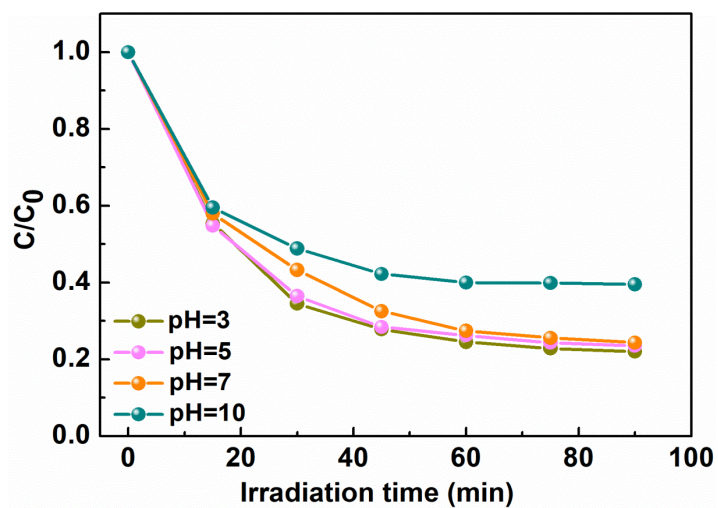


**Fig S3.** Photocatalytic degradation of tetracycline by pH of different solutions

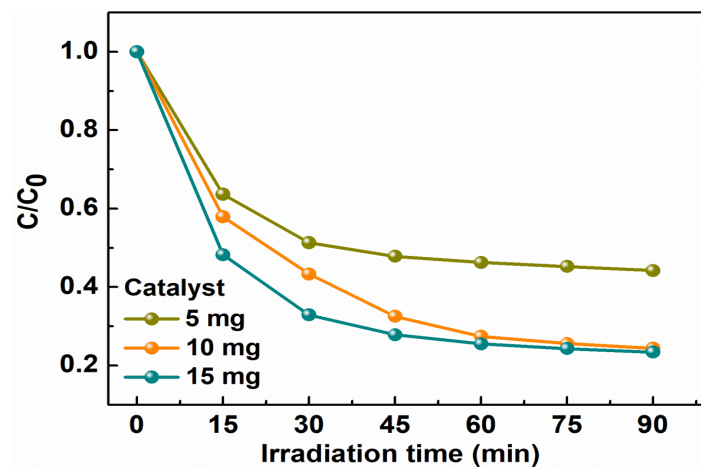


**Fig S4.** Photocatalytic degradation of tetracycline by catalysts of different quality

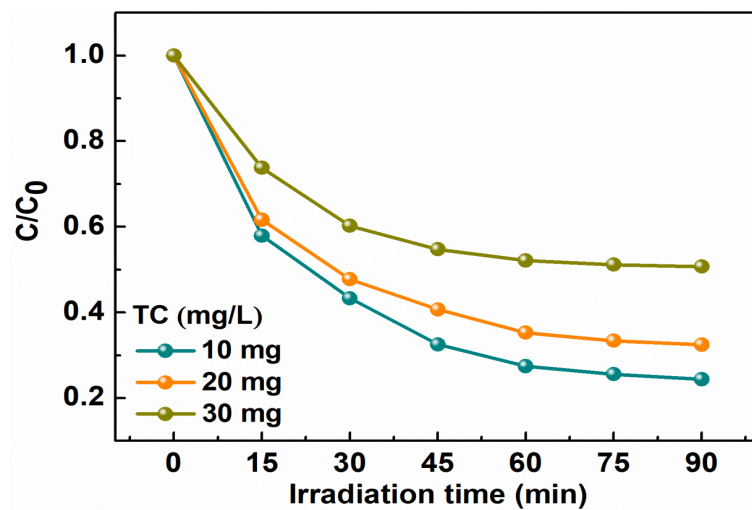
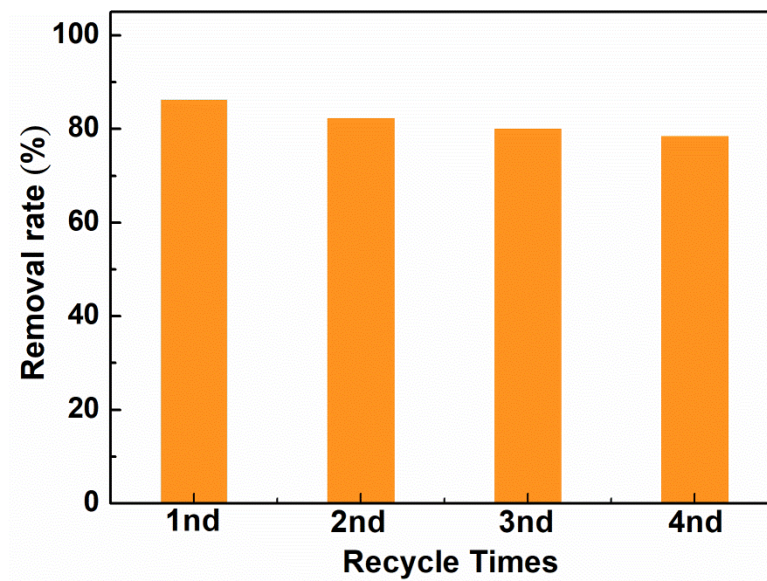


Fig S5. Photocatalytic degradation of tetracycline at different mass concentrations

**Table S2.** Comparison of photocatalytic degradation efficiency of tetracycline with OCN and other g-C<sub>3</sub>N<sub>4</sub> samples

<b>Catalyst</b>	<b>Dosage (mg)</b>	<b>Light source</b>	<b>Initial amount</b>	<b>Time (min)</b>	<b>Removal (%)</b>
GG-N <sup>[1]</sup>	2000	100W UV mercury lamp	50 mg/L	180	91.57
Ag/g-C <sub>3</sub> N <sub>4</sub> <sup>[2]</sup>	50	300W, Xenon ( $\lambda \geq 420$ nm)	20 mg/L	120	83
BiVO <sub>4</sub> /g-C <sub>3</sub> N <sub>4</sub> <sup>[3]</sup>	20	300W, Xenon	20 mg/L	60	56
CeNCN <sup>[4]</sup>	10	300W, Xenon ( $\lambda \geq 420$ nm)	10 mg/L	60	80.09
pg-C <sub>3</sub> N <sub>5</sub> <sup>[5]</sup>	40	300W, Xenon ( $\lambda \geq 420$ nm)	30 mg/L	60	83
OCN	10	300W, Xenon ( $\lambda \geq 420$ nm)	20 mg/L	60	87.7



**Fig S6.** Stability experiments of photocatalytic degradation of tetracycline of OCN

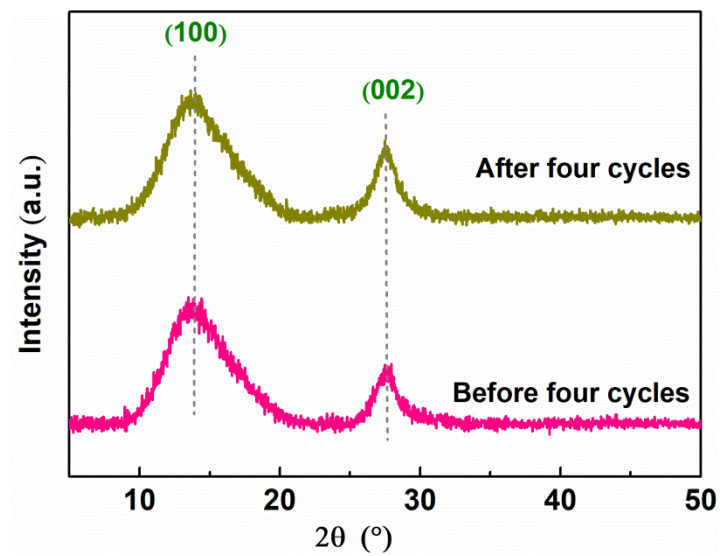
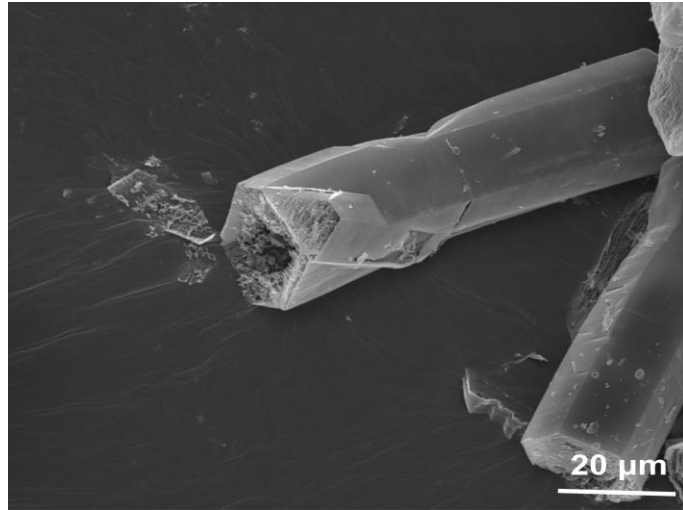
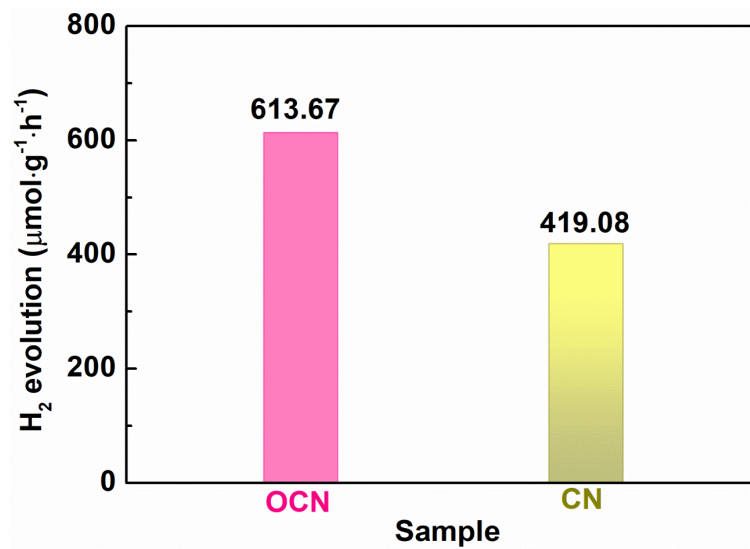


Fig S7. XRD patterns after cycles of OCN



**Fig S8.** SEM images of OCN after cycles



**Fig S9.** The rate of hydrogen production from photocatalytic water.

---

## Reference

- [1] Song Y, Zhang X, Bai C, et al. Porous spherical g-C<sub>3</sub>N<sub>4</sub>/geopolymer composite for photo-Fenton-like degradation of tetracycline hydrochloride. *Journal of Water Process Engineering*, 2025, 70: 107073.
- [2] Xu W, Lai S, Pillai S C, et al. Visible light photocatalytic degradation of tetracycline with porous Ag/graphite carbon nitride plasmonic composite: Degradation pathways and mechanism. *Journal of Colloid and Interface Science*, 2020, 574: 110-121.
- [3] Zhang X, Xie X, Li J, et al. Type II heterojunction formed between 010 or 012 facets dominated bismuth vanadium oxide and carbon nitride to enhance the photocatalytic degradation of tetracycline. *International Journal of Environmental Research and Public Health*, 2022, 19(22): 14770.
- [4] Xu F, An N, Lai C, et al. Nitrogen-doping coupled with cerium oxide loading co-modified graphitic carbon nitride for highly enhanced photocatalytic degradation of tetracycline under visible light. *Chemosphere*, 2022, 293: 133648.
- [5] Ma T, Zhang Y, Tian Y, et al. et al. Pressure-induced formation of porous g-C<sub>3</sub>N<sub>5</sub> for efficient photocatalytic degradation of tetracycline (TC). *Journal of Environmental Chemical Engineering*, 2025, 13: 116403.